

1 Cost-benefit analysis of coastal flood defence measures in the North 2 Adriatic Sea

3 Mattia Amadio¹, Arthur H. Essenfelder¹, Stefano Bagli², Sepehr Marzi¹, Paolo Mazzoli², Jaroslav Mysiak¹,
4 Stephen Roberts³

5 ¹ *Centro Euro-Mediterraneo sui Cambiamenti Climatici, Università Ca' Foscari Venezia, Italy*

6 ² *Gecosistema, Rimini, Italy*

7 ³ *The Australian National University, Canberra, Australia*

8 Abstract

9 The combined effect of ~~global~~ sea level rise and ~~local-land~~ subsidence phenomena poses a major threat to
10 coastal settlements. Coastal flooding events are expected to grow in frequency and magnitude, increasing
11 the potential economic losses and costs of adaptation. In Italy, a large share of the population and economic
12 activities are located along the coast of the peninsula, although risk of inundation is not uniformly distributed.
13 The low-lying coastal plain of Northeast Italy is the most sensitive to relative sea level changes. Over the last
14 half a century, the entire north-eastern Italian coast has experienced a significant rise in relative sea level, the
15 main component of which was land subsidence. In the forthcoming decades, ~~climate-induced~~ sea level rise is
16 expected to become the first driver of coastal inundation hazard. We propose an assessment of flood hazard
17 and risk linked with extreme sea level scenarios, both under historical conditions and sea level rise projections
18 at 2050 and 2100. We run a hydrodynamic inundation model on two pilot sites located in the North Adriatic
19 Sea along the Emilia-Romagna coast: Rimini and Cesenatico. Here, we compare alternative risk scenarios
20 accounting for the effect of planned and hypothetical seaside renovation projects against the historical
21 baseline. We apply a flood damage model developed for Italy to estimate the potential economic damage
22 linked to flood scenarios and we calculate the change in expected annual damage according to changes in the
23 relative sea level. Finally, damage reduction benefits are evaluated by means of cost-benefit analysis. Results
24 suggest an overall profitability of the investigated projects over time, with increasing benefits due to increased
25 probability of intense flooding in the next future.

26 **Key-words:** coastal inundation Italy extreme sea level rise

27 **Abbreviations:** MSL (Mean Sea Level); TWL (Total Water Level); ESL (Extreme Sea Level); SLR (Sea Level
28 Rise); VLM (Vertical Land Movements); DTM (Digital Terrain Model); EAD (Expected Annual Damage)

29 1. Introduction

30 Globally, more than 700 million people live in low-lying coastal areas (McGranahan et al. 2007), and about
31 13% of them are exposed to a 100-year return period flood event (Muis et al. 2016). On average, one million
32 people located in coastal areas are flooded every year (Hinkel et al. 2014). Coastal flood risk shows an
33 increasing trend in many places due to socio-economic growth (Bouwer 2011; Jongman et al. 2012b) and land
34 subsidence (Syvitski et al. 2009; Nicholls and Cazenave 2010), but in the near future sea level rise (SLR) will
35 likely be the most important driver of increased coastal inundation risk (Hallegatte et al. 2013; Hinkel et al.
36 2014). Evidences show that global sea level has risen at faster rates in the past two centuries compared to the
37 millennial trend (Kemp et al. 2011; Church and White 2011), topping 3.2 mm per year in the last decades
38 mainly due to ocean thermal expansion and glacier melting processes (Mitchum et al. 2010; Meyssignac and
39 Cazenave 2012). According to the IPCC projections, it is very likely that, by the end of the 21st century, the
40 SLR rate will exceed that observed in the period 1971-2010 for all Representative Concentration Pathway (RCP)
41 scenarios (IPCC 2019); yet the local sea level can have a strong regional variability, with some places

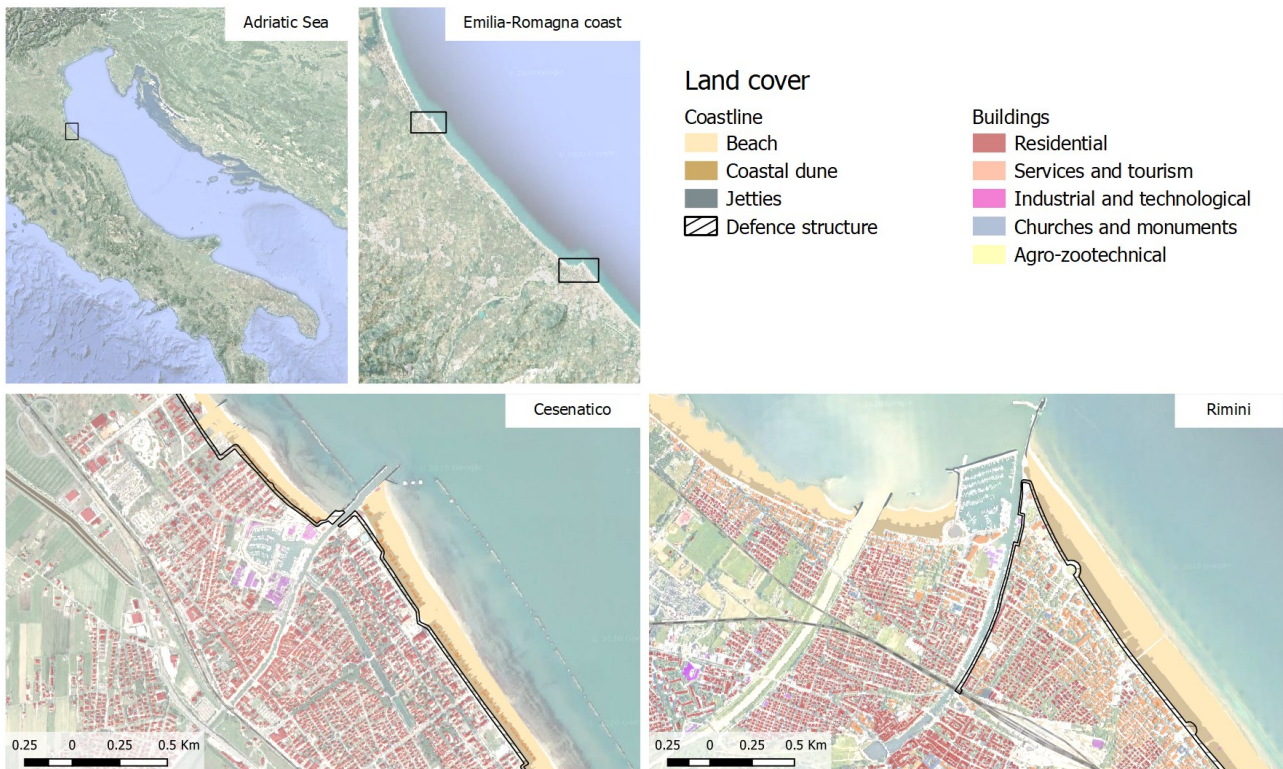
42 experiencing significant deviations from the global mean change (Stocker et al. 2013). This is particularly
43 worrisome in regions where changes in the mean sea level (MSL) are more pronounced, considering that even
44 small increases of MSL can drastically change the frequency of extreme sea level (ESL) events, leading up to
45 situations where a 100-year event may occur several times per year by 2100 (Carbognin et al. 2009, 2010;
46 Vousdoukas et al. 2017, 2018; Kirezci et al. 2020). Changes in the frequency of extreme events are likely to
47 make existing coastal protection inadequate in many places, causing a large part of the European coasts to be
48 exposed to flood hazard. Under these premises, coastal floods threaten to trigger devastating impacts on
49 human settlements and activities (Lowe et al. 2001; McInnes et al. 2003; Vousdoukas et al. 2017). In this context,
50 successful coastal risk mitigation and adaptation actions require accurate and detailed information about the
51 characterisation of coastal flood hazard and the performance of alternative coastal defence options. Cost-
52 benefit analysis (CBA) is widely used to evaluate the economic desirability of a Disaster Risk Reduction
53 (DRR) project (Jonkman et al. 2004; Mechler 2016; Price 2018). CBA helps decision-makers in evaluating the
54 efficacy of different adaptation options (Kind 2014; Bos and Zwaneveld 2017).

55 In this study, designed coastal renovation projects in the municipalities of Rimini and Cesenatico, in Italy, are
56 compared against the baseline scenario in terms of net economic benefits under changing climate conditions.
57 First, we employ the 2D-hydrodynamic ANUGA model (Roberts et al. 2015) for simulating coastal inundation
58 scenarios associated with ESL projections over the two pilot areas located along the Emilia-Romagna coast
59 (North Adriatic Sea). Flood hazard maps are produced for current conditions (2020) and future conditions
60 (2050 and 2100) by combining the local data from historical ESL events with the estimates of relative mean sea
61 level (RMSL) change for those locations. RMSL change accounts for both the eustatic global rise and the locally-
62 measured land vertical movement effect. Each inundation scenario simulated by the model is translated in
63 terms of direct economic impacts over residential areas using a locally-calibrated damage model. The
64 combination of different risk scenarios in a CBA framework allows to estimate-evaluate the economic benefits
65 brought by the project implementation in terms of avoided direct flood losses up to the end of the century.

66 2. Area of study

67 Located in the central Mediterranean Sea, the Italian peninsula has more than 78,530 km of coasts, hosting
68 around 18% of the country population (~~ISTAT~~), numerous towns and cities, industrial plants, commercial
69 harbours and touristic activities, as well as cultural and natural heritage sites. Existing country-scale estimates
70 of SLR up to the end of this century helps to identify the most critically exposed coastal areas of Italy (Lambeck
71 et al. 2011; Bonaduce et al. 2016; Antonioli et al. 2017; Marsico et al. 2017). About 40% of the coastal perimeter
72 consist of a flat coastal profile (ISPRA 2012), ~~which are the most~~ potentially more vulnerable to the impacts of
73 ESL events. The North Adriatic coastal plain is acknowledged to be the largest and most vulnerable location
74 to extreme coastal events due to the shape, morphology and low bathymetry of the Adriatic sea basin, which
75 cause water level to increase relatively fast during coastal storms (Carbognin et al. 2010; Ciavola and Coco
76 2017; Perini et al. 2017). The ESL here is driven mainly by astronomical tide, ranging about one meter in the
77 northernmost sector, ~~and~~ meteorological forcing, such as low pressure, seiches and prolonged rotational wind
78 systems, which are the main trigger of storm surge in the Adriatic basin (Vousdoukas et al. 2017; Umgieser
79 et al. 2020). In addition to that, all the coastal profile of the Padan plain shows relatively fast subsiding rates,
80 partially due to natural phenomena, but in large part linked to human activities (Carbognin et al. 2009; Perini
81 et al. 2017; Meli et al. 2021). ~~As a concurring contributing factor to coastal flood risk, the intensification of~~
82 urbanization process has led to increased exposure developed faster and more intensely along the Adriatic
83 coast during the last 50 years, with many regions building over half of the available land within 300 meters

84 ~~from the shoreline (ISPRA 2012). This study~~ We focus our analysis on two pilot sites located along the
85 Adriatic coast of Emilia-Romagna, shown in figure 1: Cesenatico and Rimini.



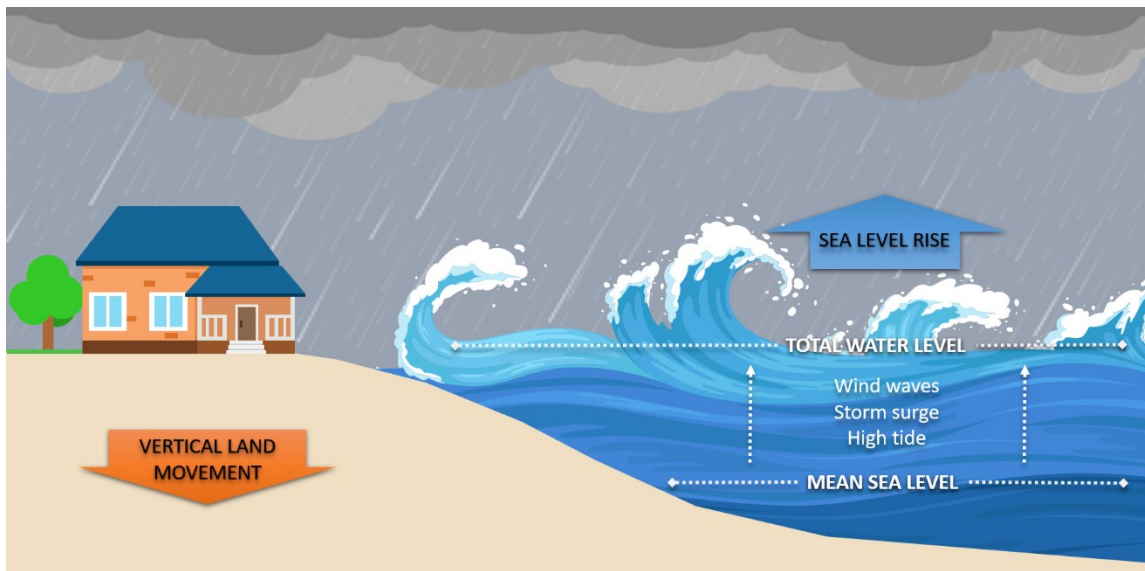
86
87 **Figure 1.** Pilot areas locations along the Emilia-Romagna coast: Cesenatico and Rimini. The coastal defence
88 structure assessed in this study are shown in black. Buildings' footprint data from Regional Environmental
89 Agency (ARPA) 2020. Basemap © Google Maps 2020.

90 The number of ~~annual~~ ESL events reported to cause impacts along the Emilia-Romagna coast shows a steady
91 increase since the second half of the past century (Perini et al. 2011), which is in part explained by to the socio-
92 economic development of the coast exposing increasing asset to flood risk. The landscape along the 130 km
93 regional coastline is almost flat, the only relief being old beach ridges, artificial embankments and a small
94 number of dunes. The coastal perimeter is delineated by a wide sandy beach that is generally protected by
95 offshore breakwaters, groins and jetties. The land elevation is often close to (or even below) the MSL, while
96 the coastal corridor is heavily urbanised. Cesenatico has about 26,000 residents, while Rimini has 150,000.
97 These port towns have a strong touristic vocation, hosting large beach resort and bathing facilities along the
98 beach and hundreds of hotels and rental housing located just behind the seaside. Both towns ~~are~~ have been
99 affected by ~~beach erosion and the regression of the coastline, and on several occasions they suffered from~~
100 coastal storms resulting in flooding of buildings and activities, beach erosion and regression of the coastline.
101 The most recent inundation events were observed in March 2010, November 2012 and February 2015. The 2015
102 event was one of the most severe ever recorded, showing with ESL values corresponding to a probability of
103 once in 100 years. It caused severe damages along the whole regional coast and, in some locations, required
104 the evacuation of people from their houses; Many buildings and roads were invaded covered by sand
105 brought by the flood wave; Touristic infrastructures near the shore were seriously damaged, and some port
106 channels overflowed the surrounding areas. The economic impact was estimated topping 7.5 M Eur (Perini et
107 al. 2015). ~~In some cases, the storm surge obstructed the river outlets causing the overflow of channels and the~~
108 ~~flooding of surrounding areas (Perini et al. 2011).~~

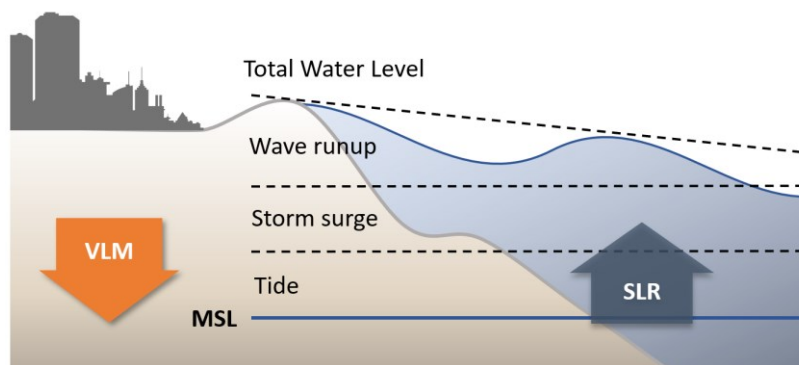
109 **3. Methodology**

110 **3.1 Components of the analysis**

111 Coastal inundation phenomena are caused by an increase of total water level (TWL), most often associated to
112 extreme sea level (ESL) events, which are generated by a combination of high astronomical tide and
113 meteorological drivers such as storm surge and wind waves (figure 2). Estimates of ESL are obtained for the
114 North Adriatic up to year 2100 by combining reference hazard scenarios derived from historical records with
115 regionalised projections of SLR (Vousdoukas et al. 2017) and local vertical land movements (VLM) rates
116 (Carbognin et al. 2009; Perini et al. 2017). Four ESL frequency scenarios, namely once in 1, 10, 100- and 250-
117 years, are considered. The hydrodynamic model ANUGA is applied to simulate the inundation of land areas
118 during ESL accounting for individual components (storm surge, tides and waves). Land morphology and
119 exposure of coastal settlements are described by high-resolution DTM and bathymetry, in combination with
120 land use and buildings footprints. The effect of hazard mitigation structures (both designed and under
121 construction) are explicitly accounted in the “defended” simulation scenario, in contrast to the baseline
122 scenario, where only existing defence structures (groins, jetties, breakwaters and sand dunes) are accounted.



123



124

125 **Figure 2.** Components of the analysis for extreme sea level events: total water level is calculated as the sum of
126 maximum tide, storm surge and wind waves runup over mean sea level. Vertical land movement and eustatic
127 sea level rise affects the mean sea level on the long run.

128 **3.2 Vertical Land Movement**

129 Vertical land movements result from a combination of slow geological processes such as tectonic activity and
130 glacial isostatic adjustment (Peltier 2004; Peltier et al. 2015), and medium-term phenomena, such as sediment

131 loading and soil compaction (Carminati and Martinelli 2002; Lambeck and Purcell 2005). The latter can greatly
132 oversize geological processes at local scale (Wöppelmann and Marcos 2012); in particular, faster subsidence
133 occurs in presence of intense anthropogenic activities such as water withdrawal and natural gas extraction
134 (Teatini et al. 2006; Polcari et al. 2018). Most of the peninsula shows a slow subsiding trend, although with
135 some local variability. An estimate of VLM rates due to tectonic activity ~~have~~has been derived from studies
136 conducted in Italy (Lambeck et al. 2011; Antonioli et al. 2017; Marsico et al. 2017; Solari et al. 2018). The North
137 Adriatic coastal plain shows the most intense long-term geological subsidence rates (about 1 mm per year),
138 increasing North to South. Yet in the last decades these rates were often greatly exceeded by ground
139 compaction rates observed by multi-temporal SAR Interferometry (Gambolati et al. 1998; Antonioli et al. 2017;
140 Polcari et al. 2018; Solari et al. 2018). Observed subsidence is about one order of magnitude faster where the
141 aquifer system has been extensively exploited for agricultural, industrial and civil use since the post-war
142 industrial boom. From the 1970s, however, with the halt of groundwater withdrawals, anthropogenic
143 subsidence has been strongly reduced or stopped, but many of the induced effects still remain (Carbognin et
144 al. 2009). Geodetic surveys carried out from 1953 to 2003 along the Ravenna coast provide evidence of a
145 cumulative land subsidence exceeding 1 m at some sites due to gas extraction activities. Average subsidence
146 rates observed for 2006-2011 along the Emilia-Romagna coast are around 5 mm/yr, exceeding 10 mm/yr in the
147 back shore of the Cesenatico and Rimini areas and topping 20-50 mm/yr in Ravenna (Carbognin et al. 2009;
148 Perini et al. 2017). Based on these current rates, we assume an average fixed annual VLM of 5 mm in both
149 Cesenatico and Rimini up to the end of the century. This remarkable difference between natural VLM rates
150 and observations would produce a dramatic effect on the estimated SLR scenarios: at present rates, Rimini
151 would see an increase of MSL by 0.15 m in 2050 and more than 0.4 m in 2100 independently from eustatic SLR.
152 Since these rates are connected with human activity, it is not possible to foresee exactly how they will change
153 in the long term.

154 3.3 Sea Level Rise

155 The long availability of tide gauge data along the N Adriatic coast allows to assess the changes in MSL ~~in~~
156 during the last century. Records from the gauge station of Marina di Ravenna show an eustatic rise of 1.2 mm
157 per year from 1890 to 2007 (Meli et al. 2021), in good agreement with the eustatic rise measured at other stations
158 in the Mediterranean Sea (Tsimplis and Rixen 2002; Carbognin et al. 2009). The projections of future MSL
159 account for sea thermal expansions from four global circulation models, estimated contributions from ice-
160 sheets and glaciers (Hinkel et al. 2014) and long-term subsidence projections (Peltier 2004). The ensemble mean
161 is chosen to represent each RCP for different time slices. The increase in the central Mediterranean basin is
162 projected to be approximately 0.2 m by 2050 and between 0.5 and 0.7 m by 2100, compared to historical mean
163 (1970-2004) (Vousdoukas et al. 2017). As agreed with stakeholders from the Municipality of Rimini, Wour
164 analyse considers the intermediate emission scenario RCP 4.5 ~~(Thomson et al. 2014)~~, projecting an increase
165 in MSL of 0.53 m at 2100. It must be noted that these projections, although downscaled for the Adriatic basin,
166 do not account for the peculiar continental characteristics of the shallow northern Adriatic sector, where the
167 hydrodynamics and oceanographic parameters partially depend on the freshwater inflow (Zanchettin et al.
168 2007).

169 3.4 Tides and meteorological forcing

170 Storm surge and strong-wind waves represents the largest contribution to TWL during an ESL event. An
171 estimation of these components is obtained for the pilot sites from the analysis of tide gauge and buoy records,
172 and from the description of historical extreme events presented in local studies (Perini et al. 2011, 2012, 2017;
173 Masina et al. 2015; Armaroli and Duo 2018). This area is microtidal: the mean neap tidal range is 30–40 cm,

174 and the mean spring tidal range is 80–90 cm. Most storms have a duration of less than 24 h and a maximum
175 significant wave height of about 2.5 m. During extreme cyclonic events, the sequence of SE wind (*Sirocco*)
176 piling the water North and E-NE wind (*Bora*) pushing waves towards the coast can generate severe inundation
177 events, with significant wave height ranging 3.3 – 4.7 m and exceptionally exceeding 5.5 m (Armaroli et al.
178 2012). Fifty significant events have been recorded from 1946 to 2010 on the ER coast, with half of them causing
179 severe impacts along the whole coast and 10 of them being associated with important flooding events (Perini
180 et al. 2017). The most severe events are found when strong winds blow during exceptional tide peaks, most
181 often happening in late autumn and winter. The event of November 1966 represents the highest ESL on
182 records, causing significant impacts along the regional coast: the recorded water level was 1.20 m above MSL,
183 and wave heights offshore were estimated around 6–7 m (Perini et al. 2011; Garnier et al. 2018). The whole
184 coastline suffered from erosion and inundation, especially in the province of Rimini. Atmospheric forcing
185 shown significant variability for the period 1960 onwards (Tsimplis et al. 2012), but there is no strong evidence
186 supporting a significant change in trend for the next future (Lionello 2012; Lionello et al. 2020; Zanchettin et
187 al. 2020). Thus, we assume the frequency and intensity of meteorological events to remain the same up to 2100.

188 3.5 Terrain morphology and coastal defence structures

189 Reliable bathymetries and topography are required in order to run the hydrodynamic modelling at the local
190 scale. Bathymetric data for the Mediterranean ~~area~~ Sea were obtained from the European Marine Observation
191 and Data Network (EMODnet) at 100 m resolution. The description of terrain morphology comes from the
192 official high-resolution LIDAR DTM (MATTM, 2019). First, we combined the coastal dataset (2 m resolution
193 and vertical accuracy of ± 0.2 m), and the inland dataset (1 m resolution and vertical accuracy ± 0.1 m) into one
194 seamless layer. Then, the DTM is supplemented with geometries of existing coastal protection elements such
195 as jetties, groins and breakwaters obtained from the digital Regional Technical Map. In Rimini, the Parco del
196 Mare is an urban renovation project which aims to improve the seafront promenade: the existing road and
197 parking lots are converted into an urban green infrastructure consisting of a concrete barrier covered by
198 vegetated sandy dunes with walking paths. This project also acts as a coastal defence system during extreme
199 sea level events. The barrier rises 2.8 meters along the southern section of the town, south of the marina; no
200 barrier is planned on the northern coastal perimeter. The Parco del Mare project, currently under construction,
201 has been taken in account in the evaluation of the “defended” scenarios by merging the barrier into the existing
202 DTM (figure 3).



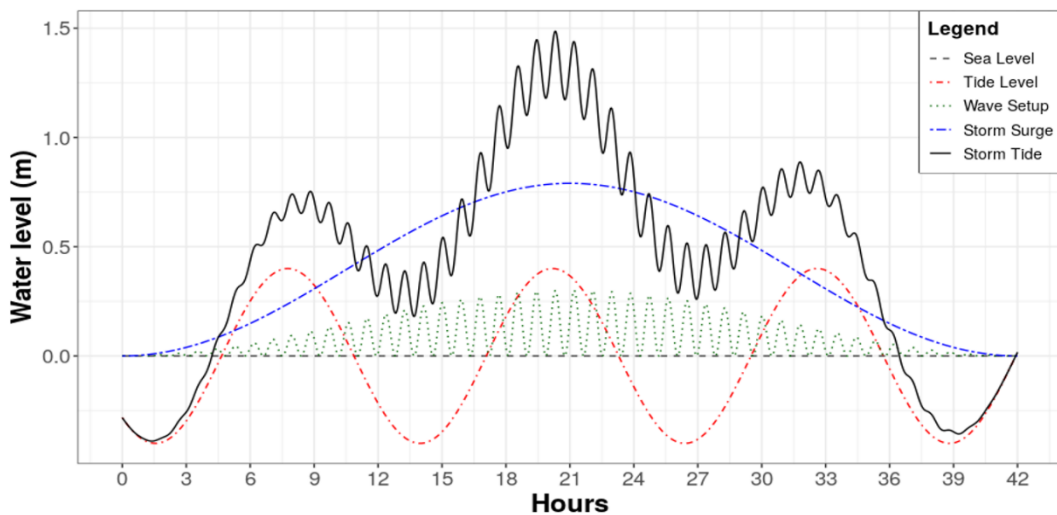
203
204 **Figure 3.** Prototype design of Parco del Mare project in Rimini. Adapted from JDS Architects.

205 In Cesenatico, the existing defence structures include a moving barriers system (*Porte Vinciane*) located on the
206 port channel, coupled with a dewatering pump which discharge the meteoric waters in the sea. The barriers
207 close automatically if the TWL surpasses 1 meter over the mean, preventing floods in the historical centre up
208 to ESL of 2.2 meters. Additional defence structures include the winter dunes, which consist of a 2.2 meter-tall

209 intermittent, non-reinforced sand barrier. In the defended scenario, we envisage a coastal defence structure
 210 similar to Parco del Mare in Rimini, spanning both ~~N~~north and ~~s~~South of the port channel with a total length
 211 of 7.8 km. A proper setup of the inundation model required to first perform some manual editing of the DTM
 212 using additional reference data (i.e. on-site observations or aerial photography) in order to produce an
 213 elevation model that realistically represent the land morphology and associated water dynamics (e.g. removal
 214 of non-existent sink holes). Bridges and tunnels are the most critical elements that required DTM correction
 215 ~~ed~~ in order to avoid misrepresentations of the water flow routing.

216 3.6 Inundation modelling

217 At the local scale, hydrodynamic models represent an efficient compromise between hydrostatic and hydraulic
 218 models, being able to perform realistic simulations of inundation phenomena and to obtain detailed
 219 information about the hazard features, while requiring a relatively fast setup and reasonable computational
 220 effort. In this study we use ANUGA, a 2D hydrodynamic model originally developed to simulate tsunami
 221 events, which is also suitable for the simulation of hydrologic phenomena such as riverine peak flows and
 222 storm surges (Roberts 2020). Being a 2D hydrodynamic model, ANUGA does not resolve vertical convection
 223 and consequently not breaking waves or 3D turbulence (e.g. vorticity), thus not considering the swash
 224 component of wave runup. The fluid dynamics in ANUGA is based on a finite-volume method for solving the
 225 shallow water wave equations, thus being based on continuity and simplified momentum equation. The
 226 model computes the total water level, the water depth, and the horizontal momentum on an irregular
 227 triangular grid based on the provided forcing conditions. ANUGA includes also an operator module that
 228 simulates the removal of sand associated with over-topping of a sand dune by sea waves, which is applied to
 229 explore scenarios where a sand dune barrier provides protection for the land behind. The operator simulates
 230 the erosion, collapse, fluidisation and removal of sand from the dune system (Kain et al. 2020); the dune
 231 erosion mechanism relies on a relationship based on Froehlich (2002). This option is enabled only in the
 232 undefended scenario for Cesenatico, where non-reinforced sand dunes are prone to erosion.



233 **Figure 4.** Total Water Level (black) as a sum of tide (red), storm surge (~~green~~blue) and wave setups (~~blue~~green)
 234 for ESL scenario 1 in 10 years.
 235

236 In our application, we estimate the TWL on the coastland is modelled at every timestep as the sum of extreme
 237 values for storm surge level (SS), wave runup-setup (W_{rs}), and max tide (T_{max}), as shown in figure 4. The
 238 maximum tidal excursion is 0.8 m, while wave height can range from 3 to almost 6 m during strong wind
 239 events, translated into a wave setup-setup on-near the shore ~~the shore~~ ranging from 0.22 to 0.65 m. Additional
 240 details are wave period (Wp , in seconds) and event duration (Time, in hours), required to estimate the

241 maximum extent of inland water propagation. Wave direction is oriented perpendicular to the coast. ~~Wave~~
 242 ~~runup is not accounted.~~ Storm surge is set to peak in the mid of the event, producing the maximum TWL value
 243 for the event. The most exceptional ESL events can last up to 3 days. Table 41 summarizes the ESL components
 244 according to the four probability scenarios identified from local historical records (Perini et al. 2017). The
 245 probability of occurrence is expressed in terms of return period (*RP*), which is the estimated average time
 246 interval between events of similar intensity. ~~Wave run-up is calculated from significant wave height.~~ The
 247 output of the simulation consists of maps representing flood extent, water depth and momentum at every time
 248 step (1 second), projected on the high-resolution DTM grid.

249 **Table 1.** components of TWL during an ESL event under historical conditions and projected conditions (2050
 250 and 2100), accounting for both eustatic SLR (RCP4.5) and average VLM rate.

<i>RP</i> (years)	Extreme event features				Historical	2050			2100		
	<i>SS</i> (m)	<i>T_{max}</i> (m)	<i>W₅</i> (m)	<i>Time</i> (h)	<i>TWL</i> (m)	<i>SLR</i> (m)	<i>VLM</i> (m)	<i>TWL</i> (m)	<i>SLR</i> (m)	<i>VLM</i> (m)	<i>TWL</i> (m)
1	0.60	0.40	0.22	32	1.2	0.14	0.19	1.55	0.53	0.44	2.2
10	0.79	0.40	0.30	42	1.5	0.14	0.19	1.82	0.53	0.44	2.5
100	1.02	0.40	0.39	55	1.8	0.14	0.19	2.14	0.53	0.44	2.8
250	1.40	0.45	0.65	75	2.5	0.14	0.19	2.83	0.53	0.44	3.5

251 3.7 Risk modelling and Expected Annual Damage

252 Direct damage to physical asset is estimated using a customary flood risk assessment approach originally
 253 developed for fluvial inundation, which is adapted to coastal flooding assuming that the dynamic of impact
 254 from long-setting floods depends on the same factors, namely: 1) hazard magnitude, and 2) size and value of
 255 exposed asset. Indirect economic losses due to secondary effects of damage (e.g. business interruption) are
 256 excluded from ~~our~~ the computation. Hazard magnitude can be defined by a range of variables, but the most
 257 important predictors of damage are water depth and the extension of the flood event (Jongman et al. 2012a;
 258 Huizinga et al. 2017). Land cover definitions and buildings footprints help to estimate the exposed capital
 259 including residential buildings, commercial and industrial activities, infrastructures, historical and natural
 260 sites. The characterization of exposed asset is built from a variety of sources, starting from land use and
 261 buildings footprints obtained from the Regional Environmental Agencies geodatabases and the Open Street
 262 Map database (Geofabrik GmbH 2018). Additional indicators about buildings characteristics are obtained
 263 from the database of the official Italian Census of 2011 (~~ISTAT~~) (ISTAT 2011), while mean construction and
 264 restoration costs per building types are obtained from cadastral estimates (CRESME 2014). ~~The asset~~
 265 ~~representation is static, meaning that the analysis does thus not accounting for changes in land use nor~~
 266 ~~population density, while allowing for the direct comparison of hazard mitigation options' results.~~ A depth-
 267 damage function ~~was~~ previously validated on empirical records (Amadio et al. 2019) and then applied in order
 268 to translate each hazard scenario into an estimate of economic risk, measured as a share of total exposed value.
 269 ~~The damage curve covers function applies only to residential and mixed-residential buildings, the area of~~
 270 ~~which represents about 93% of total exposed footprints; other types (such as e.g. harbour infrastructures,~~
 271 ~~industrial, commercial, historical monuments and churches natural sites) are excluded from risk computation.~~
 272 Abandoned or under-construction buildings are ~~also~~ excluded from the analysis. To avoid overcounting of
 273 marginally-affected buildings, we set two threshold conditions for damage calculation: flood extent must be
 274 greater than or equal to 10 m², and maximum water depth greater than or equal to 10 cm. The
 275 damage/probability scenarios are combined together as Expected Annual Damage (EAD). EAD is the damage
 276 that would occur in any given year if damages from all flood probabilities were spread out evenly over time;

277 mathematically, EAD is the integration of the flood risk density curve over all probabilities (Olsen et al. 2015),
 278 as in equation 1.

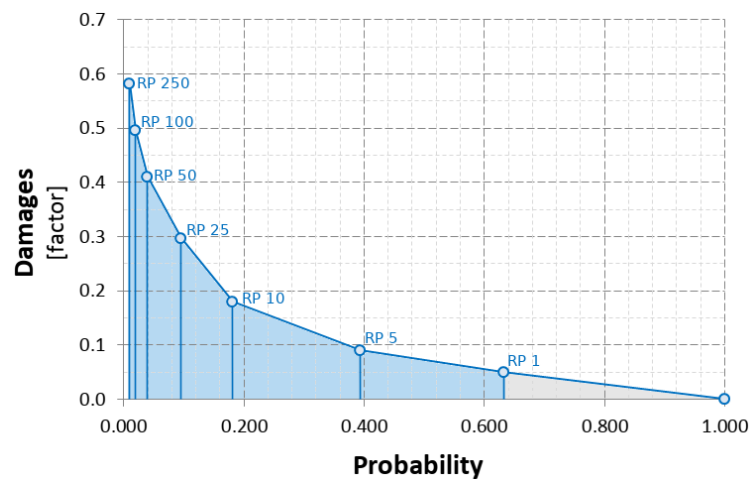
$$EAD = \int_0^1 D(p) dp \quad (1)$$

279 The integration of the curve can be solved either analytically or numerically, depending on the complexity of
 280 the damage function $D(p)$. Several different methods for numerical integration exist; we use an approach
 281 where EAD is the sum of the product of the fractions of exceedance probabilities by their corresponding
 282 damages (figure 5). We calculate $D(p)$, which is the damage that occurs at the event with probability p , by
 283 using the depth-damage function previously validated for Italy on empirical records (Amadio et al. 2019) for
 284 each hazard scenario. The exceedance probability of each event (p) is calculated based on exponential function
 285 as shown in equation 2.

$$p = 1 - e^{\left(\frac{-1}{RP}\right)} \quad (2)$$

286 Events with a high probability of occurrence and low intensity (below RP 1 year) are not simulated, and as
 287 they are assumed to not cause significant damage. This is consistent with the historical observations for the
 288 case study area, although this assumption could change with increasing MSL.

Figure 5. Schematic representation of the numerical integration of the damage function $D(p)$ with respect to the exponential probability of the hazard events. Events with a probability of occurrence higher than once in a year are expected to not cause damage (grey area).



289 3.8 Cost-Benefit Analysis

290 A CBA should include a complete assessment of the impacts brought by the implementation of the hazard
 291 mitigation option, i.e. direct and indirect, tangible and intangible impacts (Bos and Zwaneveld 2017). The
 292 project we are considering, however, has not been primarily designed for DRR purpose: instead, it is meant
 293 as an urban renovation project which aims to improve-consolidate the fruition-touristic vocation of the seafront
 294 area, to improve the quality of life and the urban environment and the urban landscape (Comune di Rimini
 295 2018). This implies some large indirect effects on the whole area, most of which are not strictly related to
 296 disaster risk management and, overall, very difficult to estimate ex-ante. Our evaluation focuses only on the
 297 benefits that are achieved-measurable in terms of reduction-in-direct flood losses reduction. Regarding the
 298 implementation costs, the CBA include-accounts for the initial investment required for setting up the
 299 adaptation measure, and operational costs through time. According to the "Parco del Mare" project funding
 300 documentation (Comune di Rimini 2019a, b, 2020, 2021a, b), the total cost of the project (to be completed during
 301 2021) is 33.3 M Eur, corresponding to The initial investment is estimated to be 5.556 M Eur per Km of length.
 302 No information is available about operational-maintenance costs of the opera, but given the nature of the
 303 project (static defense with very-low structural fragility-to-floods), we assume they will be rather small

304 compared to the initial investment. ~~We account for o~~Ordinary annual maintenance costs are accounted as 0.1%
 305 of the total cost of the ~~oper~~project. The same costs are assumed for the hypothetical barrier in Cesenatico,
 306 resulting in an initial investment cost of 43.3 M. Costs and benefit occurring in the future periods need to be
 307 discounted, as people put higher value on the present (Rose et al., 2007). This is done by adjusting future costs
 308 and benefits using an annual discount rate (r). We chose a variable rate of $r = 3.5$ for the first 50 years and $r =$
 309 3 from 2050 onward (Lowe 2008). A sensitivity analysis of discount rate is included in Annex 1. The three main
 310 decision criteria used in CBA for project evaluation are the Net Present Value (NPV), the Benefit/Cost Ratio
 311 (BCR) and the payback period. The NPV is the sum of Expected Annual Benefits (B) up to the end of the time
 312 horizon, discounted, minus the total costs for the implementation of the defense measure, which takes into
 313 account initial investment plus discounted annual maintenance costs (C). In other words, the NPV of a project
 314 equals the present value of the net benefits ($NB_i = B_i - C_i$) over a period of time (Boardman et al. 2018), as in
 315 equation (3):

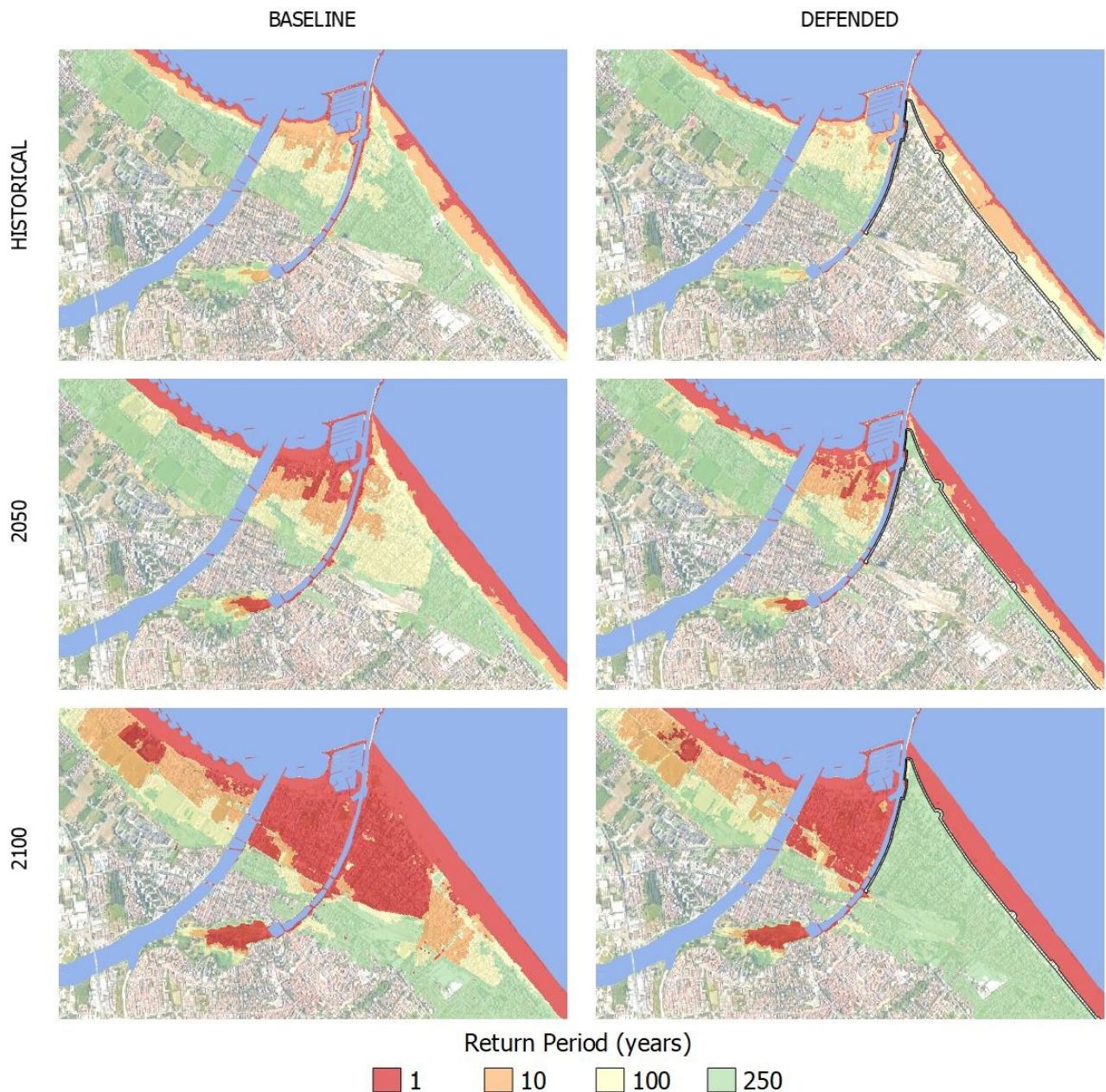
$$NPV = PV(B) - PV(C) = \sum_{t=0}^n \frac{NB_t}{(1+r)^t} \quad (3)$$

316 Positive NPV means that the project is economically profitable. The BCR is instead the ratio between the
 317 benefits and the ~~costs~~; a BCR larger than 1 means that the benefits of the project exceed the costs on the long
 318 term and the project is considered profitable. The payback period is the number of years required for the
 319 discounted benefits to equal the total costs.

320 4. Results

321 4.1 Inundation scenarios

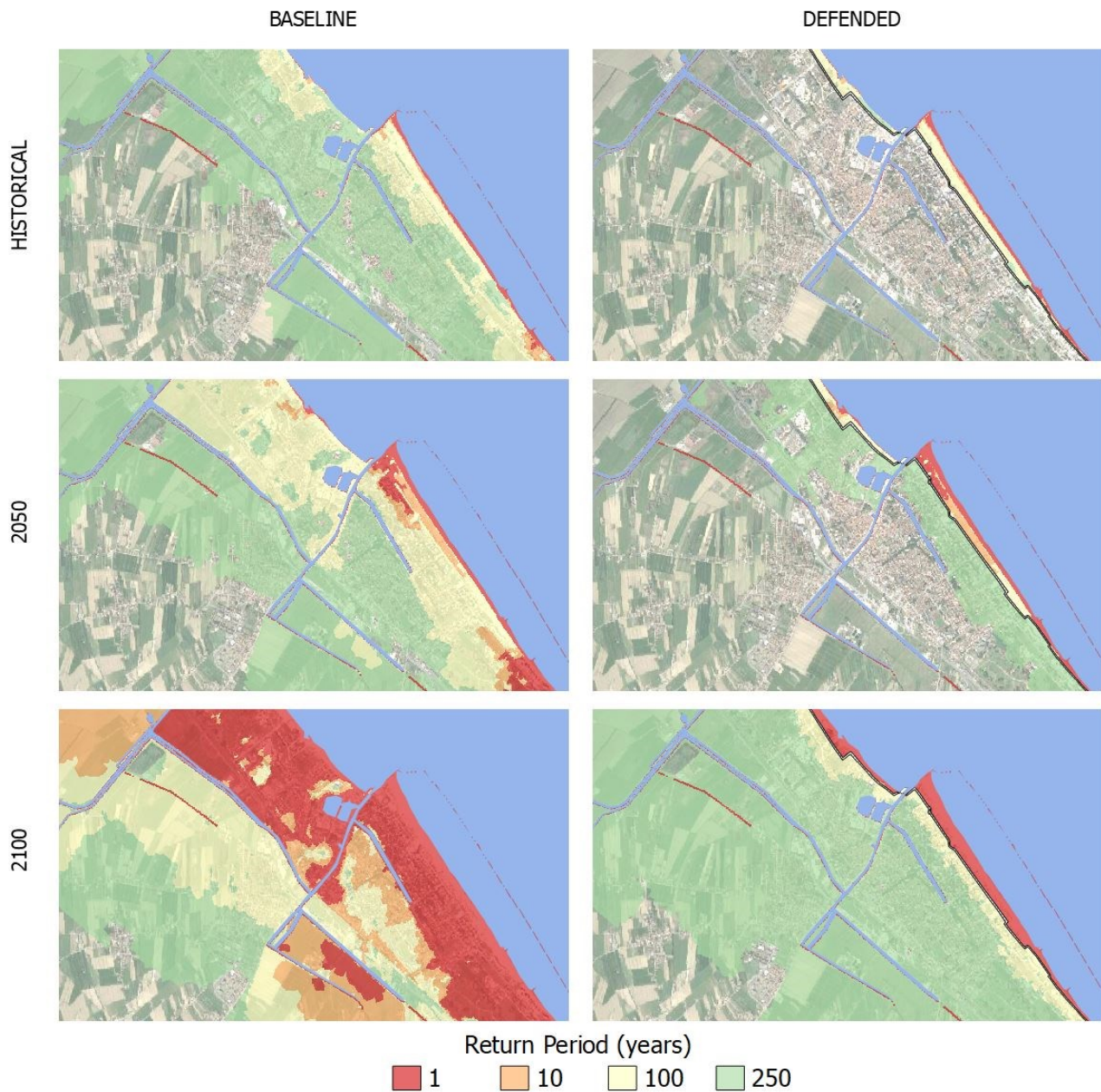
322 Once the setup is completed, the hydrodynamic model performs relatively fast: each simulation is carried at
 323 half speed compared to real ~~timeity, requiring ; that means, it takes~~ about 24 hours to simulate a 12 h event.
 324 Parallel simulations for the same area can run on a multicore processor, improving the efficiency of the process.
 325 The output of the hydrodynamic model consists of a set of inundation simulations that include several hazard
 326 intensity variables in relation to flood extent: water depth, flow velocity, and duration of submersion. ESL
 327 scenarios are then summarized into static maps, each one representing the maximum value reached by hazard
 328 intensity variables at grid cell level (about 1 meter) during the whole simulated event. The flood extents
 329 corresponding to each RP scenario are shown for Rimini (figure ~~65~~) and Cesenatico (figure ~~76~~).



330

331 **Figure 6.** Rimini, extent of land affected by flood according to frequency of occurrence of ESL event up to 2100
 332 for the baseline [left] and the defended scenario [right]. Basemap © Google Maps 2020.

333 In Rimini, the Parco del Mare barrier produces benefits in terms of avoided damage in the south-eastern part
 334 of the town (high-density area) for ESL events with a probability return period of up to 1 in 100 years or less.
 335 The north-western part and the marina are outside of the defended area; being these areas are therefore subject
 336 to, they suffer the same a similar amount of flooding in both across scenarios are not affected by the coastal
 337 renovation project. In all the simulations, the buildings located behind the marina are the firsts to be flooded.
 338 In fact, the new and the old port channels located on both sides of the marina represent a hazard hotspot: as
 339 shown in the maps, the failure of the eastern channel, which has a relatively low elevation, is likely to cause
 340 the water to flood the eastern part of the town, even during inundation events that would not surpass the
 341 beach perimeter. In the defended scenarios, where both the coastal and the canal barriers are enabled, the flood
 342 extent in the SE urban area becomes almost zero for ESL events with a probability of once in 100 years, even
 343 when accounting for SLR up to 2100. Under more exceptional ESL conditions (RP 250 in 2100), the barrier is
 344 surmounted, generating a flood extent similar to the baseline scenario for the same occurrence probability.



345

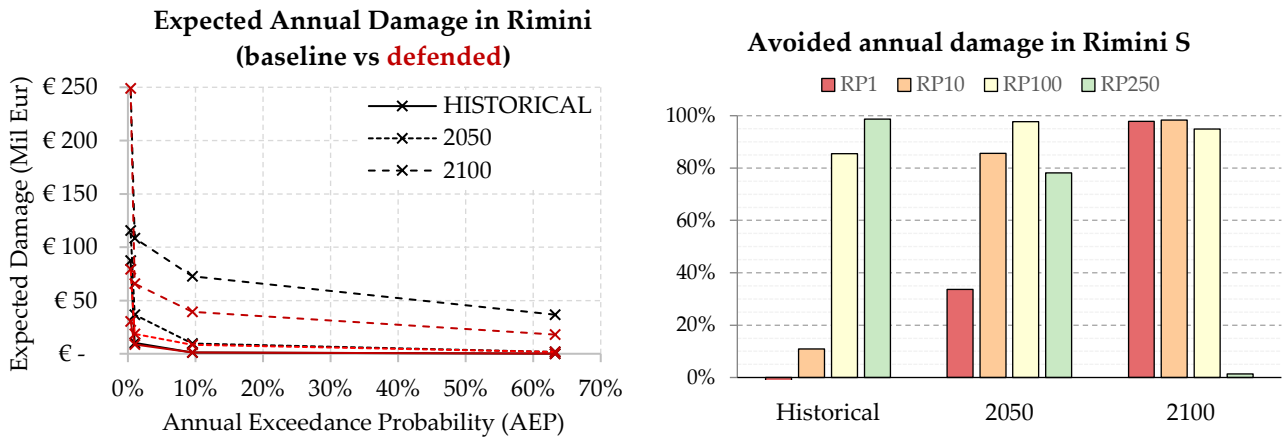
346 **Figure 7.** Cesenatico, extent of land affected by flood according to frequency of occurrence of ESL event up to
 347 2100 for the baseline [left] and the defended scenario [right]. Basemap © Google Maps 2020.

348 In Cesenatico, a barrier designed similarly to Parco del Mare could provide significant reduction of flood
 349 extents under most hazard scenarios. Its effectiveness would be greater than in Rimini thanks to the
 350 complementary movable barrier system in use, which seals the port channel allowing to wall off the whole
 351 coastal perimeter, reducing the chance of water ingress in the urban area. In contrast, the erodible winter
 352 dune in the baseline defense scenario can only hold the heavy sea for shorter, less intense ESL events, and
 353 becomes ineffective with more exceptional, long-lasting events; at 2050 and 2100, the winter dune gets
 354 surmounted and dismantled by sea waves for scenario RP250 years (mid- and low-left maps).

355 **4.2 Expected Annual Damage**

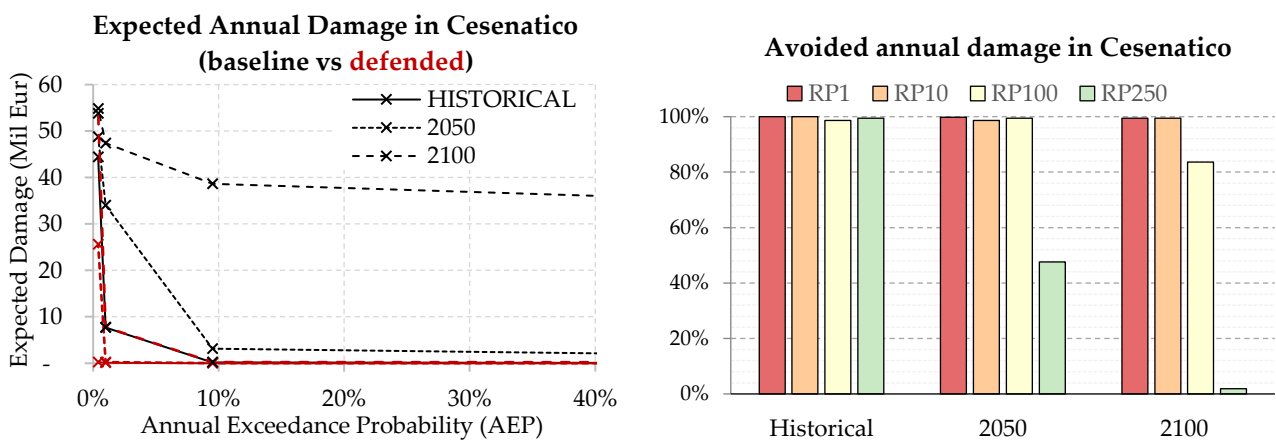
356 The ~~estimate of Expected Annual Damage expected economic impacts~~ is calculated as a function of maximum
 357 exposed value, and water depth ~~is summarized as Expected Annual Damage in figure 7, left chart~~. In Rimini,
 358 the EAD grows from around 650 thousand Eur under historical conditions to 2.8 million Eur in 2050 and more

359 than 32.3 million Eur in 2100. With less severe events (up to RP 100 years), the risk remains mostly confined
 360 around the marina area (outside the protection offered by the reinforced dune) producing an EAD below 10
 361 thousand Eur; with higher more intense water levels ESL scenarios (i.e. RP 250 years), the benefits of the dune
 362 barrier protecting the southern part of the town Rimini become more evident, avoiding about 65% of the EAD.
 363 The damage avoided by the barrier in the southern sector (Rimini S) in the defended area grows almost linearly
 364 with the increase of EAD under future projections of sea level rise: under the defended hypothesis, the EAD
 365 is reduced on average by 45% (figure 8, left). The project produces benefit up to ESL RP250 years in 2100,
 366 where a projected TWL of 3.5 meters would cause the surmounting of the barrier, reducing the benefits to almost
 367 zero (figure 78, right).



368
 369 **Figure 8.** Rimini: Expected Annual Damage (EAD) according to undefended scenario up to 2100 [left]; EAD
 370 reduction in the South part of the town thanks to hazard mitigation offered by the coastal barrier [right].

371 In Cesenatico, the average EAD for the undefended scenario grows from around 270 thousand Eur under
 372 historical conditions, to 1.7 million Eur in 2050 and almost 26 million Eur in 2100. In our simulations, the
 373 designed barrier defence structure (a static 2.8 m barrier with height of 2.8 m along 7.8 km of coast) was-is able
 374 to avoid most of the damage inflicted to residential buildings (figure 98, rightleft). The measure becomes less
 375 efficient for the most extreme scenarios in 2050 and 2100, when the increase in TWL causes the surmounting
 376 of the barrier (figure 9, right). This assessment does not account for the beach resorts and bathing facilities,
 377 which are located along the barrier or between the barrier and the sea, and thus are equally exposed in both
 378 the baseline and the defended scenario; they would likely represent an additional 7-25% of the baseline
 379 damage.



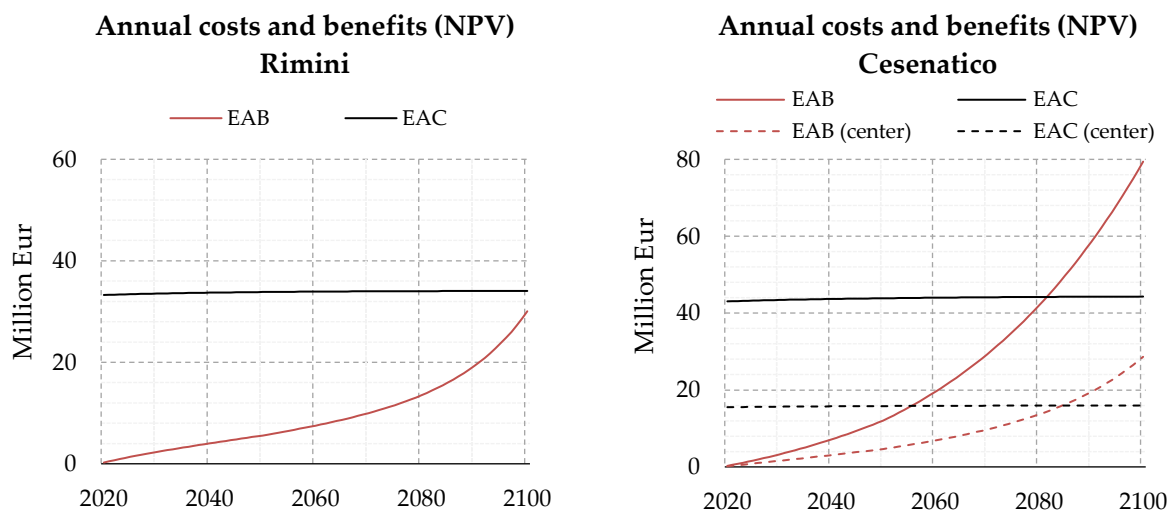
380
 13

381 **Figure 9.** Cesenatico: Expected Annual Damage (EAD) according to undefended scenario up to 2100 [left];
 382 EAD reduction thanks to hazard mitigation offered by the coastal barrier [right].

383 **4.3 Cost-Benefit Analysis**

384 ~~The EAD estimates of avoided due to direct flood impacts obtained for both the baseline and the defended~~
 385 ~~scenarios enable allows~~ are accounted in ~~for to running~~ a DRR-oriented CBA to evaluate the feasibility of
 386 mitigation measures in terms of NPV, BCR and payback period for the two time-horizons (30 years and 80
 387 years). ~~The assessment does not measure the indirect benefits brought in terms of urban renovation, which are~~
 388 ~~the primary focus of Parco del Mare project, measuring, instead, only the direct benefits in terms of direct~~
 389 ~~flood damage reduction.~~ In figure 109, the Expected Annual Benefits (EAB) grow at faster rate approaching
 390 2100 in both sites, because of the larger expected damages from more intense, less frequent flood events. The
 391 cost of defence implementation is repaid by avoided damage after about 470 years in Cesenatico and after 90
 392 years in Rimini. ~~In Cesenatico benefits grow proportionally to costs, so that the payback time does not change~~
 393 ~~when considering a section of the town or the whole coastal perimeter.~~ At 2100, the BCR is 0.982 for Rimini
 394 and 1.866 for Cesenatico. ~~These results clearly indicate, suggesting~~ an overall profitability of the defence
 395 structure implementation over the long term ~~for Cesenatico. For the case of the municipality of Rimini, further~~
 396 ~~investigation is required in order to holistically account for the non-DRR benefits of the seafront renovation~~
 397 ~~project. For instance, factors such as the potential reduction in indirect losses in terms of capital and labour~~
 398 ~~productivity due to less frequent and less intense flooding events, and the potential increase in tourism and~~
 399 ~~well-being of citizens due to renewed urban landscape, are factors that could be accounted for in a holistic the~~
 400 ~~CBA analysis and would likely return a shorter payback period.~~

401 In order to better understand the potential benefits of the mitigation measures over different areas of the
 402 ~~considered two municipalities, we compare the~~ The results in terms of CBR ~~do not differ much when~~
 403 ~~comparing the CBA~~ over a selection of exposed records corresponding to the town higher-density area (i.e.
 404 Cesenatico historical center). Table 2 summarizes the metrics of the assessment for different area extent
 405 selections. ~~As shown in Table 2, Results do not differ much when comparing the CBA over different areas of~~
 406 ~~the municipalities. In Cesenatico benefits grow proportionally to costs, so that the payback time does not~~
 407 ~~change when considering a section of the town or the whole coastal perimeter. Moreover, As specified~~
 408 ~~discussed earlier, this assessment does not measure the benefits brought in terms of urban renovation, which~~
 409 ~~are the primary focus of Parco del Mare project, but only measuring, instead, the direct benefits in terms of~~
 410 ~~direct flood damage reduction.~~



411

412 **Figure 10.** Cumulated flood defence costs and expected benefits at Net Present Value for Rimini (left) and
 413 Cesenatico (right).

415 **Table 2.** Summary of CBA for planned or designed seaside defence project in Rimini (all town and south
 416 section only) and Cesenatico (all town and center only) over a time horizon of 30 and 80 years (2020 to 2050
 417 and 2020 to 2100).

Metrics	Rimini				Cesenatico			
	All town		South only		All town		Center only	
	2050	2100	2050	2100	2050	2100	2050	2100
Baseline EAD [M EUR]	2.8	32	0.5	14.6	1.7	25.9	0.5	12.4
Defended EAD [M EUR]	2.4	17	0.1	0.9	0.1	0.4	0.1	0.4
Expected Annual Benefits [M EUR]	0.43	15	0.4	13.7	1.6	25.5	0.4	11.9
Sum of EAB (discounted) [M EUR]	5.6	30	4.1	27.8	12.0	79.4	4.7	28.6
Sum of EAC (discounted) [M EUR]	336.68	346.90	363.68	364.90	473.48	474.93	157.18	176.30
Net Present Value [M EUR]	-	-64.80	-	-96.31	-315.38	315.51	-121.24	121.63
	2831.0		2932.8					
	3		6					
Benefit-Cost ratio [-]	0.165	0.882	0.124	0.8175	0.285	1.6679	0.2730	1.7966

418 5. Conclusion

419 In this study we addressed coastal inundation risk scenarios ~~and measures on over~~ two coastal ~~sites towns~~
 420 located along the North Adriatic coastal plain of Italy, which is projected to become increasingly exposed to
 421 ESL events due to changes in MSL induced by SLR and subsidence phenomena. Both locations are expected
 422 to suffer increasing economic losses from ~~to coastal inundation triggered by extreme sea level~~ these events
 423 unless effective coastal adaptation measures are put in place. To understand the ~~impacts of~~ upcoming
 424 ~~impacts ESL events~~ and the potential benefits of designed coastal projects, we run a CBA comparing the
 425 baseline and the defended scenario in terms of flood losses over residential buildings, which represent the
 426 largest share of exposed buildings' footprints (93%). The defended scenario accounts for the effect of a coastal
 427 barriers based on the design of the "Parco del Mare", an urban renovation project under construction in
 428 Rimini. The same type of defence structure is envisaged ~~and its effects simulated~~ along the coastal perimeter
 429 of the nearby town of Cesenatico. First, we characterised reference ESL events in terms of frequency and
 430 intensity based on local historical observations; then, we projected ESL scenarios to 2050 and 2100, accounting
 431 for the combined effect of eustatic SLR and subsidence rates on the TWL, as obtained from existing local
 432 studies. We produced flood hazard maps estimating maximum flood ~~water extent and~~ water depth ~~and~~
 433 ~~velocity~~ using a high-resolution hydrodynamic model able to replicate the physics of the inundation process.
 434 The hazard maps were fed to the damage model in order to calculate the expected annual damage for both
 435 baseline and defended scenarios. An increase in damage is expected for both urban areas from 2020 to 2100:
 436 in Cesenatico the EAD grows by a factor 96, in Rimini by a factor 49.

437 The results obtained from the CBA on both locations show growing profitability of present project investment
 438 over time, associated with the increase of expected annual damage from intense ESL events: the EAD under
 439 the baseline hypothesis is expected to increase by 3.5-fold in 2050, up to 10-fold in 2100. The benefits brought
 440 by the coastal defence project become much larger in the second half of the century: the EAB grows 6.1-fold in
 441 Rimini, 6.5-fold in Cesenatico, from 2050 to 2100. Avoided losses are expected to match the project
 442 implementation costs after about ~~70-40~~ years in Cesenatico and 90 years in Rimini. Benefits are found to
 443 increase proportionally to costs; the payback period in Cesenatico is the same considering either an investment
 444 on the protection of the whole town or only part of it. Further assessments of these renovation projects should
 445 look to measure the indirect and spill-over effects over the local economy brought by the project, ~~and~~ possibly

446 accounting also for the intangible benefits and scenarios of exposure change. The results are calculated in
447 relation to emission scenario RCP4.5; compared to RCP8.5 at 2050, the difference in SLR contribution would
448 be too negligible small (~0.05 m), while a to realistically affect the damage output and the CBA. At 2100, the
449 difference between the two emission scenarios is larger (around 0.2 m), thus additional scenario analysis areis
450 suggested in future research.

451 Data availability

452 Mattia Amadio, & Arthur H. Essenfelder. (2021). Coastal flood inundation scenarios over Cesenatico and
453 Rimini: hazard and risk for Business as Usual and Defended options [Data set]. Natural Hazard and Earth
454 System Sciences. <http://doi.org/10.5194/nhess-2020-414>

455 **Authors contribution**

456 MA, AHE and SB conceptualized the study and designed the experiments. AHE carried out the coastal hazard
457 modelling. SR advised the model setup and calculation. SB and PM provided required data and expertise
458 about the case study areas. MA performed the economic risk modelling and wrote the manuscript. SM
459 supported the CBA calculations. JM and SB managed the funding acquisition and project supervision. All co-
460 authors have reviewed the manuscript.

461 **Acknowledgment**

462 The research leading to this paper received funding through the projects CLARA (EU's Horizon 2020 research
463 and innovation programme under grant agreement 730482), SAFERPLACES (Climate-KIC innovation
464 partnership) and EUCP – European Climate Prediction system under grant agreement 776613. We want to
465 thank Luisa Perini for her kind support.

466 **References**

- 467 Amadio M, Scorzini AR, Carisi F, et al (2019) Testing empirical and synthetic flood damage models: the case
468 of Italy. *Nat Hazards Earth Syst Sci* 19:661–678 . doi: 10.5194/nhess-19-661-2019
- 469 Antonioli F, Anzidei M, Amorosi A, et al (2017) Sea-level rise and potential drowning of the Italian coastal
470 plains: Flooding risk scenarios for 2100. *Quat Sci Rev* 158:29–43 . doi: 10.1016/j.quascirev.2016.12.021
- 471 Armaroli C, Ciavola P, Perini L, et al (2012) Critical storm thresholds for significant morphological changes
472 and damage along the Emilia-Romagna coastline, Italy. *Geomorphology* 143–144:34–51 . doi:
473 10.1016/j.geomorph.2011.09.006
- 474 Armaroli C, Duo E (2018) Validation of the coastal storm risk assessment framework along the Emilia-
475 Romagna coast. *Coast Eng* 134:159–167 . doi: 10.1016/j.coastaleng.2017.08.014
- 476 Boardman AE, Greenberg DH, Vining AR, Weimer DL (2018) *Cost-Benefit Analysis*. Cambridge University
477 Press
- 478 Bonaduce A, Pinardi N, Oddo P, et al (2016) Sea-level variability in the Mediterranean Sea from altimetry
479 and tide gauges. *Clim Dyn* 47:2851–2866 . doi: 10.1007/s00382-016-3001-2
- 480 Bos F, Zwaneveld P (2017) *Cost-Benefit Analysis for Flood Risk Management and Water Governance in the*
481 *Netherlands: An Overview of One Century*. SSRN Electron J. doi: 10.2139/ssrn.3023983
- 482 Bouwer LM (2011) Have disaster losses increased due to anthropogenic climate change? *Bull Am Meteorol*
483 *Soc*. doi: 10.1175/2010BAMS3092.1

- 484 Carbognin L, Teatini P, Tomasin A, Tosi L (2010) Global change and relative sea level rise at Venice: What
485 impact in term of flooding. *Clim Dyn* 35:1055–1063 . doi: 10.1007/s00382-009-0617-5
- 486 Carbognin L, Teatini P, Tosi L (2009) The impact of relative sea level rise on the Northern Adriatic Sea coast,
487 Italy. *WIT Trans Ecol Environ* 127:137–148 . doi: 10.2495/RAV090121
- 488 Carminati E, Martinelli G (2002) Subsidence rates in the Po Plain, northern Italy: the relative impact of
489 natural and anthropogenic causation. *Eng Geol* 66:241–255 . doi: 10.1016/S0013-7952(02)00031-5
- 490 Church JA, White NJ (2011) Sea-Level Rise from the Late 19th to the Early 21st Century. *Surv Geophys*
491 32:585–602 . doi: 10.1007/s10712-011-9119-1
- 492 Ciavola P, Coco G (eds) (2017) Coastal storms: processes and impacts. Wiley-Blackwell
- 493 Comune di Rimini (2018) Parco del Mare Sud - Strategia per la rigenerazione urbana
- 494 Comune di Rimini (2019a) Deliberazione originale di giunta comunale N. 99 del 11/04/2019
- 495 Comune di Rimini (2019b) Deliberazione originale di giunta comunale N. 118 del 02/05/2019
- 496 Comune di Rimini (2020) Deliberazione originale di giunta comunale N. 128 del 26/05/2020
- 497 Comune di Rimini (2021a) Deliberazione originale di giunta comunale N. 19 del 19/01/2021
- 498 Comune di Rimini (2021b) Deliberazione originale di giunta comunale N. 20 del 19/01/2021
- 499 CRESME (2014) Definizione dei costi di (ri)costruzione nell’edilizia
- 500 Froehlich DC (2002) IMPACT Project Field Tests 1 and 2: “Blind” Simulation. 1–18
- 501 Gambolati G, Giunta G, Putti M, et al (1998) Coastal Evolution of the Upper Adriatic Sea due to Sea Level
502 Rise and Natural and Anthropic Land Subsidence. 1–34 . doi: 10.1007/978-94-011-5147-4
- 503 Garnier E, Ciavola P, Spencer T, et al (2018) Historical analysis of storm events: Case studies in France,
504 England, Portugal and Italy. *Coast Eng* 134:10–23 . doi: 10.1016/j.coastaleng.2017.06.014
- 505 Geofabrik GmbH (2018) OpenStreetMap data extracts
- 506 Hallegatte S, Green C, Nicholls RJ, Corfee-Morlot J (2013) Future flood losses in major coastal cities. *Nat*
507 *Clim Chang*. doi: 10.1038/nclimate1979
- 508 Hinkel J, Lincke D, Vafeidis AT, et al (2014) Coastal flood damage and adaptation costs under 21st century
509 sea-level rise. *Proc Natl Acad Sci*. doi: 10.1073/pnas.1222469111
- 510 Huizinga J, Moel H De, Szewczyk W (2017) Global flood depth-damage functions : Methodology and the
511 Database with Guidelines
- 512 IPCC (2019) IPCC Special Report on the Ocean and Cryosphere in a Changing Climate
- 513 ISPRA (2012) Mare e ambiente costiero. Temat Primo Piano - Annu dei dati Ambient 2011 259–322
- 514 ISTAT (2011) 15° censimento della popolazione e delle abitazioni
- 515 Jongman B, Kreibich H, Apel H, et al (2012a) Comparative flood damage model assessment: towards a
516 European approach. *Nat Hazards Earth Syst Sci* 12:3733–3752
- 517 Jongman B, Ward PJ, Aerts JCJH (2012b) Global exposure to river and coastal flooding: Long term trends
518 and changes. *Glob Environ Chang*. doi: 10.1016/j.gloenvcha.2012.07.004
- 519 Jonkman SN, Brinkhuis-Jak M, Kok M (2004) Cost benefit analysis and flood damage mitigation in the
520 Netherlands. *Heron* 49:95–111
- 521 Kain CL, Lewarn B, Rigby EH, Mazengarb C (2020) Tsunami Inundation and Maritime Hazard Modelling
522 for a Maximum Credible Tsunami Scenario in Southeast Tasmania, Australia. *Pure Appl Geophys*
523 177:1549–1568 . doi: 10.1007/s00024-019-02384-0

- 524 Kemp AC, Horton BP, Donnelly JP, et al (2011) Climate related sea-level variations over the past two
525 millennia. *Proc Natl Acad Sci U S A* 108:11017–11022 . doi: 10.1073/pnas.1015619108
- 526 Kind JM (2014) Economically efficient flood protection standards for the Netherlands. *J Flood Risk Manag*
527 7:103–117 . doi: 10.1111/jfr3.12026
- 528 Kirezci E, Young IR, Ranasinghe R, et al (2020) Projections of global-scale extreme sea levels and resulting
529 episodic coastal flooding over the 21st Century. *Sci Rep* 10:1–12 . doi: 10.1038/s41598-020-67736-6
- 530 Lambeck K, Antonioli F, Anzidei M, et al (2011) Sea level change along the Italian coast during the Holocene
531 and projections for the future. *Quat Int* 232:250–257 . doi: 10.1016/j.quaint.2010.04.026
- 532 Lambeck K, Purcell A (2005) Sea-level change in the Mediterranean Sea since the LGM: Model predictions
533 for tectonically stable areas. In: *Quaternary Science Reviews*. Pergamon, pp 1969–1988
- 534 Lionello P (2012) The climate of the Venetian and North Adriatic region: Variability, trends and future
535 change. *Phys Chem Earth* 40–41:1–8 . doi: 10.1016/j.pce.2012.02.002
- 536 Lionello P, Barriopedro D, Ferrarin C, et al (2020) Extremes floods of Venice: characteristics, dynamics, past
537 and future evolution. *Nat Hazards Earth Syst Sci* 1–34 . doi: 10.5194/nhess-2020-359
- 538 Lowe J (2008) Intergenerational wealth transfers and social discounting: Supplementary Green Book
539 guidance. HM Treasury, London 3–6
- 540 Lowe J, Gregory J, Flather R (2001) Changes in the occurrence of storm surges around the United Kingdom
541 under a future climate scenario using a dynamic storm surge model driven by the Hadley Centre
542 climate models. *Clim Dyn* 18:179–188
- 543 Marsico A, Lisco S, Lo Presti V, et al (2017) Flooding scenario for four Italian coastal plains using three
544 relative sea level rise models. *J Maps* 13:961–967 . doi: 10.1080/17445647.2017.1415989
- 545 Masina M, Lamberti A, Archetti R (2015) Coastal flooding: A copula based approach for estimating the joint
546 probability of water levels and waves. *Coast Eng* 97:37–52 . doi: 10.1016/j.coastaleng.2014.12.010
- 547 McGranahan G, Balk D, Anderson B (2007) The rising tide: Assessing the risks of climate change and human
548 settlements in low elevation coastal zones. *Environ Urban*. doi: 10.1177/09562478070706960
- 549 McInnes KL, Walsh KJE, Hubbert GD, Beer T (2003) Impact of sea-level rise and storm surges in a coastal
550 community. *Nat Hazards* 30:187–207 . doi: 10.1023/A:1026118417752
- 551 Mechler R (2016) Reviewing estimates of the economic efficiency of disaster risk management: opportunities
552 and limitations of using risk-based cost–benefit analysis. *Nat Hazards* 81:2121–2147 . doi:
553 10.1007/s11069-016-2170-y
- 554 Meli M, Olivieri M, Romagnoli C (2021) Sea-level change along the emilia-romagna coast from tide gauge
555 and satellite altimetry. *Remote Sens* 13:1–26 . doi: 10.3390/rs13010097
- 556 Meyssignac B, Cazenave A (2012) Sea level: A review of present-day and recent-past changes and variability.
557 *J. Geodyn*. 58:96–109
- 558 Mitchum GT, Nerem RS, Merrifield MA, Gehrels WR (2010) Modern Sea-Level-Change Estimates. In:
559 *Understanding Sea-Level Rise and Variability*. Wiley-Blackwell, Oxford, UK, pp 122–142
- 560 Muis S, Verlaan M, Winsemius HC, et al (2016) A global reanalysis of storm surges and extreme sea levels.
561 *Nat Commun* 7:1–11 . doi: 10.1038/ncomms11969
- 562 Nicholls RJ, Cazenave A (2010) Sea-level rise and its impact on coastal zones. *Science* (80-) 328:1517–1520 .
563 doi: 10.1126/science.1185782
- 564 Olsen AS, Zhou Q, Linde JJ, Arnbjerg-Nielsen K (2015) Comparing methods of calculating expected annual
565 damage in urban pluvial flood risk assessments. *Water (Switzerland)* 7:255–270 . doi: 10.3390/w7010255
- 566 Peltier WR (2004) Global Glacial Isostasy and the surface of the ice-age Earth: the ICE-5G (VM2) Model and

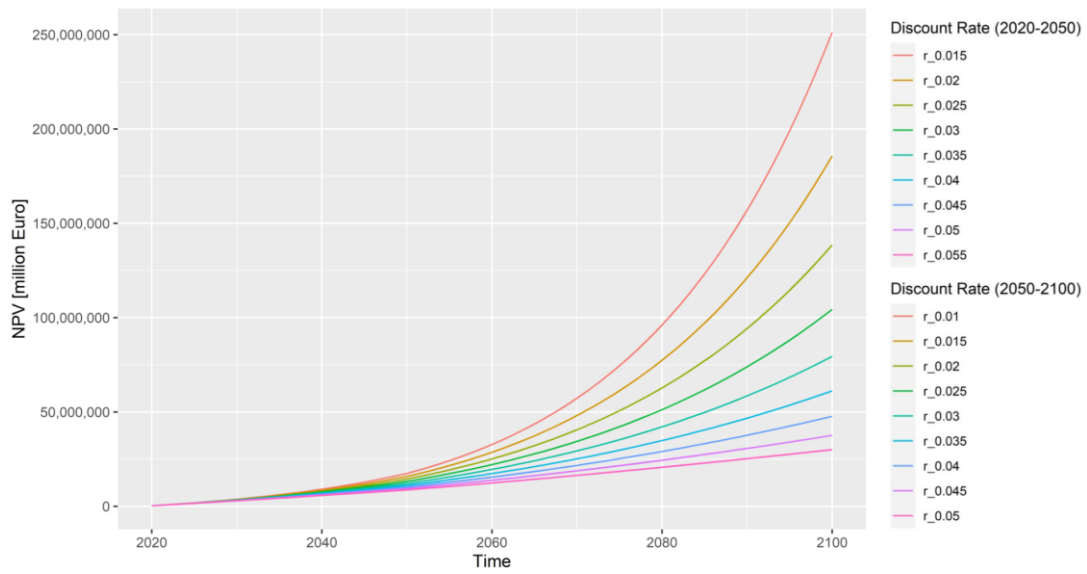
- 567 GRACE. *Annu Rev Earth Planet Sci* 32:111–149 . doi: 10.1146/annurev.earth.32.082503.144359
- 568 Peltier WR, Argus DF, Drummond R (2015) Space geodesy constrains ice age terminal deglaciation: The
569 global ICE-6G_C (VM5a) model. *J Geophys Res Solid Earth* 120:450–487 . doi: 10.1002/2014JB011176
- 570 Perini L, Calabrese L, Deserti M, et al (2011) Le mareggiate e gli impatti sulla costa in Emilia-Romagna 1946-
571 2010
- 572 Perini L, Calabrese L, Lorito S, Luciani P (2015) Il rischio da mareggiata in Emilia-Romagna: l'evento del 5-6
573 Febbraio 2015. *Geol* 53:8–17
- 574 Perini L, Calabrese L, Luciani P, et al (2017) Sea-level rise along the Emilia-Romagna coast (Northern Italy) in
575 2100: Scenarios and impacts. *Nat Hazards Earth Syst Sci* 17:2271–2287 . doi: 10.5194/nhess-17-2271-2017
- 576 Perini L, Calabrese L, Salerno G, Luciani P (2012) Mapping of flood risk in Emilia-Romagna coastal areas.
577 *Rend Online Soc Geol Ital* 21:501–502 . doi: 10.13140/2.1.1703.7766
- 578 Polcari M, Albano M, Montuori A, et al (2018) InSAR monitoring of Italian coastline revealing natural and
579 anthropogenic ground deformation phenomena and future perspectives. *Sustain* 10:4–7 . doi:
580 10.3390/su10093152
- 581 Price R (2018) Cost-effectiveness of disaster risk reduction and adaptation to climate change. 1–21
- 582 Roberts S (2020) ANUGA - Open source hydrodynamic / hydraulic modelling
- 583 Roberts S, Nielsen O, Gray D, Sexton J (2015) ANUGA User Manual
- 584 Solari L, Del Soldato M, Bianchini S, et al (2018) From ERS 1/2 to Sentinel-1: Subsidence Monitoring in Italy
585 in the Last Two Decades. *Front Earth Sci* 6: . doi: 10.3389/feart.2018.00149
- 586 Stocker TF, Dahe Q, Plattner G-K, et al (2013) Technical Summary. In: Stocker TF, Qin D, Plattner G-K, et al.
587 (eds) *Climate Change 2013: The Physical Science Basis. Contribution of Working Group I to the Fifth*
588 *Assessment Report of the Intergovernmental Panel on Climate Change*. Cambridge University Press,
589 Cambridge, United Kingdom and New York, NY, USA., pp 33–115
- 590 Syvitski JPM, Kettner AJ, Overeem I, et al (2009) Sinking deltas due to human activities. *Nat Geosci*. doi:
591 10.1038/ngeo629
- 592 Teatini P, Ferronato M, Gambolati G, Gonella M (2006) Groundwater pumping and land subsidence in the
593 Emilia-Romagna coastland, Italy: Modeling the past occurrence and the future trend. *Water Resour Res*
594 42: . doi: 10.1029/2005WR004242
- 595 Tsimplis MN, Raicich F, Fenoglio-Marc L, et al (2012) Recent developments in understanding sea level rise at
596 the Adriatic coasts. *Phys Chem Earth* 40–41:59–71 . doi: 10.1016/j.pce.2009.11.007
- 597 Tsimplis MN, Rixen M (2002) Sea level in the Mediterranean Sea: The contribution of temperature and
598 salinity changes. *Geophys Res Lett* 29:51-1-51–4 . doi: 10.1029/2002gl015870
- 599 Umgiesser G, Bajo M, Ferrarin C, et al (2020) The prediction of floods in Venice: methods, models and
600 uncertainty. *Nat Hazards Earth Syst Sci* 1–47 . doi: 10.5194/nhess-2020-361
- 601 Vousdoukas MI, Mentaschi L, Feyen L, Voukouvalas E (2017) Extreme sea levels on the rise along Europe's
602 coasts. *Earth's Futur* 5:1–20 . doi: 10.1002/eff2.192
- 603 Vousdoukas MI, Mentaschi L, Voukouvalas E, et al (2018) Global probabilistic projections of extreme sea
604 levels show intensification of coastal flood hazard. *Nat Commun* 9:1–12 . doi: 10.1038/s41467-018-
605 04692-w
- 606 Wöppelmann G, Marcos M (2012) Coastal sea level rise in southern Europe and the nonclimate contribution
607 of vertical land motion. *J Geophys Res Ocean* 117: . doi: 10.1029/2011JC007469
- 608 Zanchettin D, Bruni S, Raicich F, et al (2020) Review article: Sea-level rise in Venice: historic and future
609 trends. *Nat Hazards Earth Syst Sci Discuss* 1–56 . doi: 10.5194/nhess-2020-351

610 Zanchettin D, Traverso P, Tomasino M (2007) Observations on future sea level changes in the Venice lagoon.
611 Hydrobiologia. doi: 10.1007/s10750-006-0416-5

612

613 **Appendix A Annex 1**

614 A sensitivity analysis is carried out on the discount rate. Figure A1 below shows how the NPV changes with
615 discount rate r ranging from 1.5% to 5.5% (2020 to 2050) and 1% to 5% (2050-2100).



616

617 **Figure A1.** Sensitivity analysis of NPV using a variable discount rate.